V.H.1 Fuel Cells Systems Analysis

Rajesh K. Ahluwalia (Primary Contact),
Xiaohua Wang
Argonne National Laboratory
9700 South Cass Avenue
Argonne, IL 60439
Phone: (630) 252-5979
Email: walia@anl.gov

DOE Manager
Nancy Garland
Phone: (202) 586-5673
Email: Nancy.Garland@ee.doe.gov

Project Start Date: October 1, 2003
Project End Date: Project continuation and direction determined annually by DOE

Overall Objectives

- Develop a validated model for automotive fuel cell systems, and use it to assess the status of the technology.
- Conduct studies to improve performance and packaging, to reduce cost, and to identify key R&D issues.
- Compare and assess alternative configurations and systems for transportation and stationary applications.
- Support DOE/U.S. DRIVE automotive fuel cell development efforts.

Fiscal Year (FY) 2013 Objectives

- Validate the stack model for fuel cells with 3M's nano-structured thin-film (NSTF) catalysts in membrane electrode assemblies (MEAs).
- Develop a model for air management system with Roots compressors and expanders.
- Validate the cross-flow humidifier model using data for a prototype unit with Gore's sandwich membranes.
- Update the performance of the reference automotive fuel cell system using recent data for system components.

Technical Barriers

This project addresses the following technical barriers from the Fuel Cells section of the Fuel Cell Technologies Office Multi-Year Research, Development, and Demonstration Plan:

(B) Cost

(C) Performance

Technical Targets

This project is conducting system level analyses to address the following DOE 2020 technical targets for automotive fuel cell power systems operating on direct hydrogen:

- Energy efficiency: 60% at 25% of rated power
- $Q/\Delta T$: 1.45 kW/°C
- Power density: 850 W/L for system, 2,500 W/L for stack
- Specific power: 650 W/kg for system, 2,000 W/kg for stack
- Transient response: 1 s from 10% to 90% of maximum flow
- Start-up time: 30 s from –20°C and 5 s from +20°C ambient temperature
- Precious metal content: 0.125 g/kW (rated)

FY 2013 Accomplishments

- Collaborated with 3M in taking cell data to validate the model for NSTF catalyst-based MEAs and stacks.
- Developed a kinetic model for the oxygen reduction reaction on PtCoMn/NSTF catalyst.
- Developed a kinetic model for hydrogen oxidation and hydrogen evolution reactions on PtCoMn/NSTF catalyst.
- Developed a neural network model for mass transfer overpotentials in PtCoMn/NSTF cathode catalyst.
- Developed and validated a model for mass transfer overpotentials in PtCoMn/NSTF anode catalyst because of nitrogen buildup.
- Conducted a preliminary study to investigate the impact of the heat rejection constraint ($Q/\Delta T$) on fuel cell system cost and performance.

INTRODUCTION

While different developers are addressing improvements in individual components and subsystems in automotive fuel cell propulsion systems (i.e., cells, stacks, balance-of-plant components), we are using modeling and analysis to address issues of thermal and water management, design-point and part-load operation, and component-, system-, and vehicle-level efficiencies and fuel economies. Such analyses are essential for effective system integration.

APPROACH

Two sets of models are being developed. The GCtool software is a stand-alone code with capabilities for design, off-design, steady state, transient, and constrained optimization analyses of fuel cell systems (FCSs). A companion code, GCtool-ENG, has an alternative set of models with a built-in procedure for translation to the MATLAB®/Simulink® platform commonly used in vehicle simulation codes, such as Autonomie.

RESULTS

In FY 2013, we continued to collaborate with 3M to obtain reference performance data on 50-cm^2 active area single cells using MEAs that consisted of 3M 24-µm membrane (850 equivalent weight), ternary $Pt_{0.68}Co_{0.3}Mn_{0.02}$ NSTF catalyst, and 3M gas diffusion layers (GDLs) made by applying a hydrophobic treatment to a backing paper and a micro-porous layer [1]. The Pt loading was 0.050 $mg.cm^{-2}$ in the anode and 0.054, 0.103, 0.146, or 0.186 $mg.cm^{-2}$ in the cathode. All cells were first conditioned using a "thermal cycling" process, described in detail in Steinbach et al. [2], which consisted of repeated temperature and voltage cycles over a period of 2-3 days until stable performance was reached. The polarization curves were obtained for different temperatures (30-90°C), inlet pressures (1-2.5 atm), inlet relative humidities (25-100%), and stoichiometries for the cathode (1.5-10) and the anode (1.2-5) by running galvanodynamic scans at cell current densities varying from 0.02 to 2 $A{\cdot}cm^{-2}$. The cell was held for 120 s at each current step and the cell voltage and the high-frequency resistance (from alternating current impedance measurements) were recorded every 5 s. Prior to the start of the experiments, for each cell, the electrochemical surface area (ECSA) was determined by cyclic voltammetry, the hydrogen crossover current density and cell short resistance were determined by measuring the plateau currents, and the mass activity of Pt was measured in H_2/O_2 at 80°C, 1-atm reactant H_2 and O_2 pressures, and 100% relative humidity (RH).

Oxygen Reduction Reaction (ORR) Kinetics

We used the polarization data at low current densities (<0.5 $A{\cdot}cm^{-2}$) to determine the kinetic constants for the ORR on PtCoMn/NSTF catalyst. We found that the kinetic data could be correlated with a single Tafel equation and a transfer coefficient that is a function of the relative humidity [3]. The correlation indicates a 0.36 order for the O_2 partial pressure, 39.5 $kJ{\cdot}mol^{-1}$ activation energy for the temperature dependence, and an additional 0.9 order for RH dependence. The calculated mass activities and specific activities at 0.9 V ohmic resistance corrected cell voltage, 1 atm H_2 and O_2 partial pressures, 80°C and 100% RH agree well with the measured values of 0.13-0.25 $A{\cdot}mg_{Pt}^{-1}$ and 1.7-2.0 $mA{\cdot}cm_{Pt}^{-2}$ for the cells with different Pt loading.

Hydrogen Oxidation Reaction (HOR) Kinetics

We analyzed the kinetics of the HOR and hydrogen evolution reaction (HER) on PtCoMn/NSTF catalyst by operating the 50-cm^2 cells in H_2 pump mode with supersaturated feeds at 45-90°C and 0.7-2.5 atm H_2 partial pressures. The results showed that the HOR and HER are completely reversible, and that both of these reactions can be described by the same Butler-Volmer kinetics with first-order dependence on the H_2 partial pressure [4]. The specific exchange current density for the 2-electron HOR/HER on the NSTF ternary catalyst, derived from the measured polarization curves, is 489 $mA{\cdot}cm_{Pt}^{-2}$ at 80°C and 1-atm H_2 partial pressure. The temperature dependence of the exchange current density is consistent with an activation energy of 38.9 $kJ.mol^{-1}$. Compared to dispersed Pt/C catalyst with an ultralow 0.003 $mg.cm^{-2}$ Pt loading, the HOR kinetics on NSTF catalyst with 0.05-0.10 $mg.cm^{-2}$ Pt loading was 60-110% faster on an area-specific basis, but it was slower on a mass basis. The measured HOR/HER kinetics is a function of the state of the catalyst in that the specific exchange current density increased by 460% when the anode catalyst was conditioned with the same protocol normally used for the cathode catalyst.

Cathode Mass Transfer

We used the measured polarization curves, HFRs, mass activities, ECSAs, and H_2 crossover current density to develop, train, and validate an artificial neural network for cathode mass transfer and ohmic overpotentials. We determined the weights and biases for the multilayer perceptron feed-forward network with one hidden layer and 20 neurons using hyperbolic tangent as the activation function. Figure 1 compares the modeled artificial neural network mass transfer overpotentials with the data derived from four series of tests that varied cell temperature, cell pressure, inlet relative humidity and cathode Pt loading. In agreement with data, the model shows increasing mass transfer overpotentials (η_{mc}) as the cell temperature (Figure 1a) or pressure (Figure 1b) is lowered while maintaining exit RH at 100%. The dependence of η_{mc} on inlet RH is more complex in Figure 1c since the highest mass transfer overpotentials do not occur under wettest conditions. Similar to data for dispersed Pt/C, the NSTF catalyst system also shows higher mass transfer overpotentials as the Pt loading is decreased (Figure 1d).

Anode Mass Transfer

A special series of tests was designed to determine the anode mass transfer overpotentials (η_{ma}) due to N_2 buildup. These tests were run with 0-75% N_2 in feed H_2 and variable anode stoichiometry and cathode dew points. The temperature was varied between 70 to 85°C at 1.5-2.5 atm. Figure 2 shows the effect of N_2 buildup on anode overpotentials estimated as the differences in measured cell

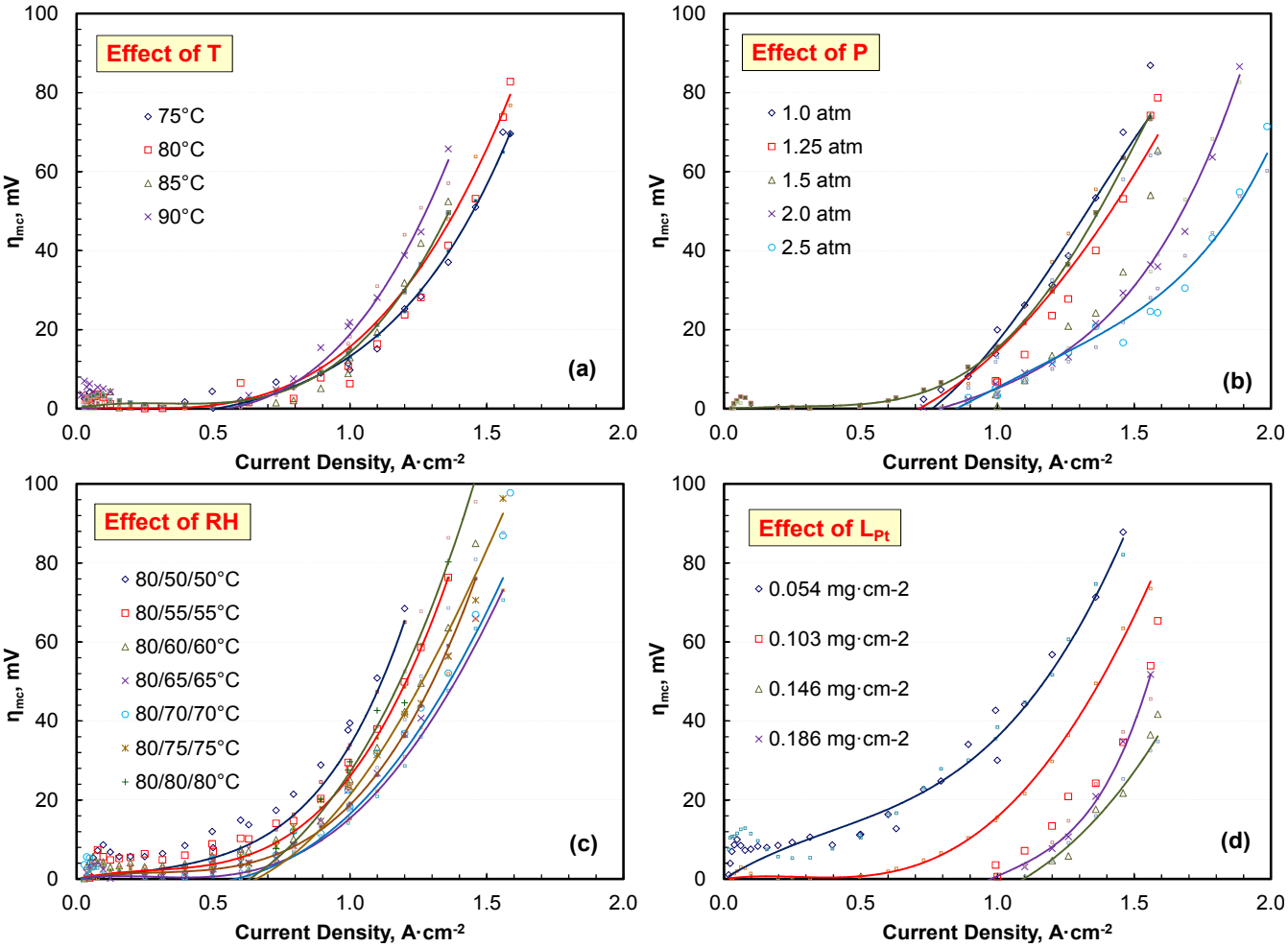

FIGURE 1. Validation of the artificial neural network model for cathode mass transfer overpotentials. The variables are: a) cell temperature and inlet RH (1.5 atm, 0.104 mg_{Pt}·cm^{-2} in cathode); b) inlet pressure and inlet RH (80°C, 0.104 mg_{Pt}.cm^{-2} in cathode); c) inlet relative humidity (1.5 atm, 80°C, 0.104 mg_{Pt}.cm^{-2} in cathode); and d) cathode Pt loading (1.5 atm, 80°C).

voltages with and without N_2 in feed H_2. The data in Figure 2 were used to derive and correlate anode mass transfer coefficient as a function of Reynolds number, pressure, temperature, and H_2 fraction. The correlation was used to develop a model to determine performance losses due to HOR kinetics, anode mass transfer and decrease in Nernst potential with N_2 buildup. The results from this model are shown as solid lines and compared with test data in Figure 2.

Model Validation

The above correlations for ORR kinetics, HOR kinetics, cathode mass transfer, and anode mass transfer have been incorporated in a multi-nodal model that determines the current density distribution along the cell, concentration (H_2, O_2, N_2, H_2O vapor) fields in the counter-flowing anode and cathode streams, liquid water movement across the catalyst layers and GDLs, water transport across the membrane, and temperature fields. The model was calibrated against the cell voltages measured in the 50-cm^2 performance tests. The calibration is shown as a parity plot in Figure 3 for the performance data at 1.5, 2.5, and 3 atm for different temperatures, RH, cathode/anode stoichiometries, and Pt loadings in cathode catalyst. In general, the model results compare well with the experimental data ($R^2 > 0.987$) and the agreement is even better at higher pressures.

System Performance

The cell model is being used to evaluate the performance of an NSTFC stack in an 80-kW_{net} fuel cell system (see [5,6] for system configuration). The initial focus of the study is on the effect of the heat rejection target ($Q/\Delta T = 1.45$) on system cost and performance. Here Q is the waste heat produced in the stack and ΔT is the difference between the coolant stack outlet temperature and the ambient (heat sink) temperature taken as 40°C. Figure 4 summarizes the results from an optimization study that minimized the system cost [7] subject to the constraint of specified $Q/\Delta T$. The variables to be optimized were coolant outlet temperature,

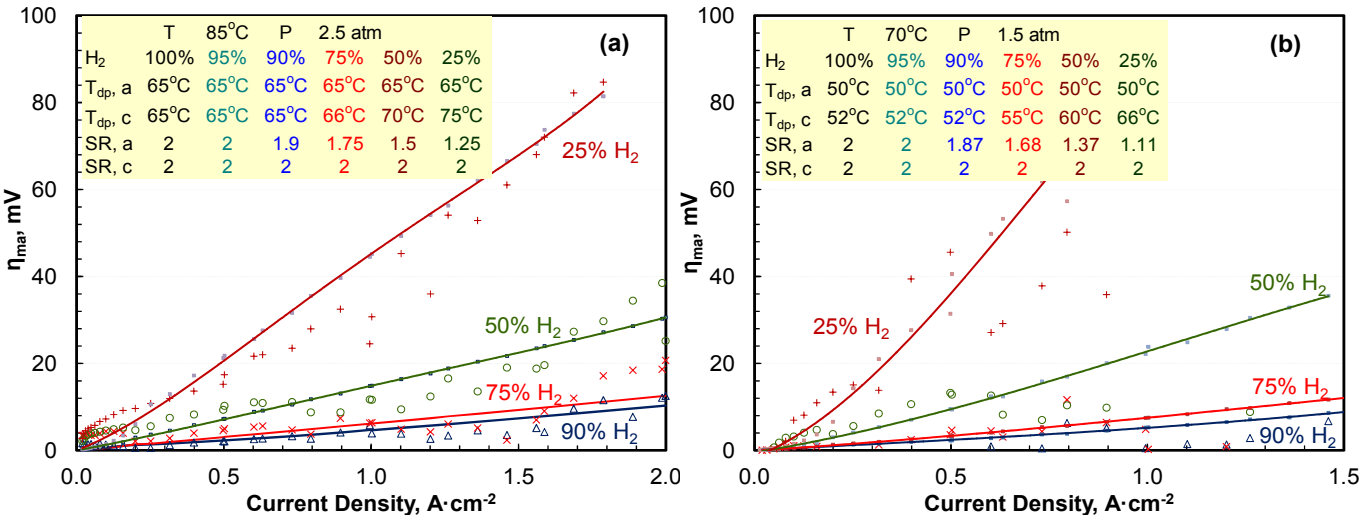

FIGURE 2. Anode mass transfer overpotentials in ternary NSTF catalyst: a) data at 85°C and 2.5 atm; b) data at 70°C and 1.5 atm anode stoichiometry (SR_a) and anode/cathode dew points (T_{dp}) are functions of the feed composition.

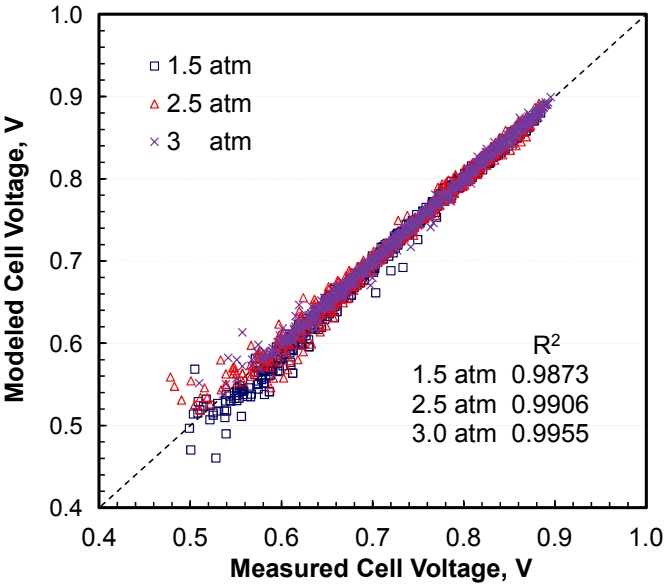

FIGURE 3. Validation of the cell model using all the data at 1.5, 2.5 and 3 atm inlet pressures.

dew-point temperature of cathode air at stack inlet, cathode stoichiometry and Pt loading in cathode. Stack inlet pressure was treated as a study parameter. As listed in the legend, Pt loading in anode (L_{Pt}), rise in coolant temperature across the stack (ΔT_c), and anode stoichiometries were held constant. Illustrative results in Table 1 for 2.5-atm stack inlet pressure indicate that constraining Q/ΔT to smaller values requires increasing system efficiency at rated power which in turn results in higher cell voltage, lower power density (not listed), and increased Pt content (g/kW) and system cost ($/kW). Meeting Q/ΔT=1.45 kW/°C target also required that the coolant temperature be raised to the 95°C allowable limit and this also contributed to decrease in stack power density. For comparison, Table 1 includes the Pt content and system cost for the same system efficiency but without the Q/ΔT constraint. For the same system efficiency, the differences in Pt content and system cost in Table 1 with and without the Q/ΔT constraint are measures of the decrease in power density because of the elevated stack temperature (ΔT effect). The differences in Pt content and system cost in Table 1 and Figure 4 for different Q/ΔT are measures of the decrease in power density because of higher cell voltages (Q effect).

CONCLUSIONS AND FUTURE DIRECTIONS

- The mass activities calculated from the ORR kinetic model are in agreement with the 0.13-0.25 $A \cdot mg^{-1}$ activities measured for the ternary NSTF catalyst with 0.054-0.186 $mg \cdot cm^{-2}$ Pt loadings.
- Specific exchange current densities for HOR/HER on ternary NSTF catalyst with 0.05 $mg \cdot cm^{-2}$ Pt loading are 60-110% higher than on Pt/C at much lower Pt loadings. The HOR/HER activities can be increased significantly if anode catalyst is conditioned more completely.
- As in dispersed Pt/C catalysts, the artificial neural network model indicates higher mass transfer overpotentials at lower Pt loadings in the ternary NSTF catalyst.
- A multi-variable optimization study showed that elevated stack temperatures and higher cell voltages are required as the stack operating conditions are changed to accommodate the target of 1.45 kW/°C Q/ΔT with resulting penalty in Pt content (g/kW) and system cost ($/kW).

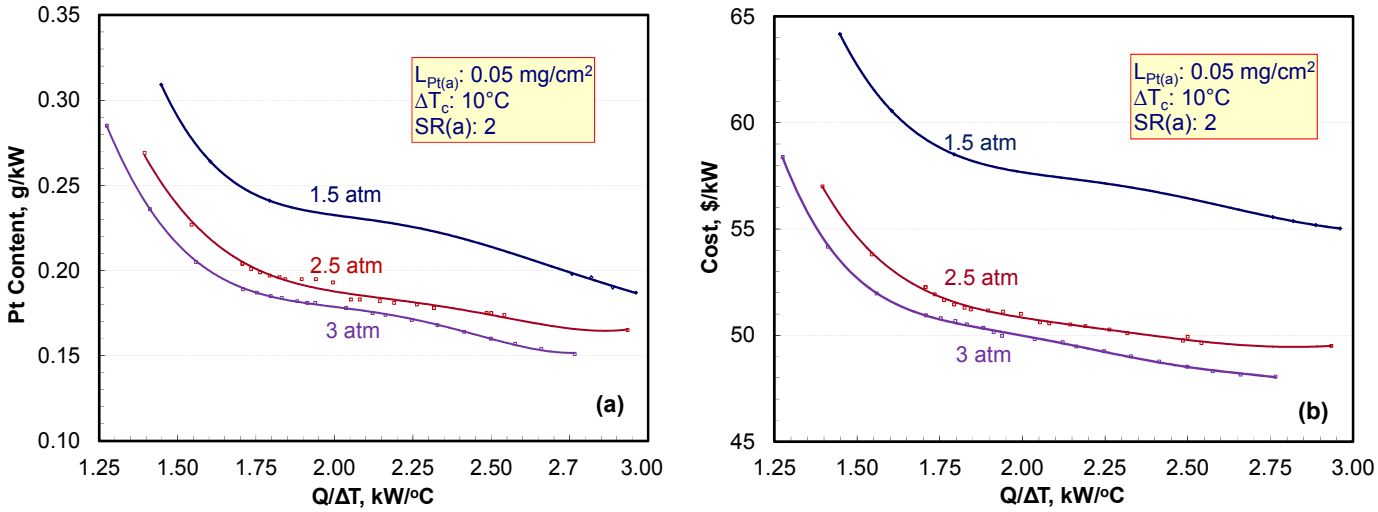

FIGURE 4. Effect of Q/ΔT constraint on system performance: a) Pt content; b) system cost.

TABLE 1. Effect of Q/ΔT target on system performance, 2.5 atm stack inlet pressure, 40°C ambient temperature

Minimum cost subject to Q/ΔT constraint, 95°C maximum stack temperature, 40°C ambient temperature					Minimum cost for given system efficiency (40°C)	
Q/ΔT	System	Cell V	Pt Content	Cost	Pt Content	Cost
kW/°C	Eff.,%	mV	g/kW	$/kW	g/kW	$/kW
3.0	40	574	0.17	49.5	0.17	49.5
1.7	45	640	0.20	52.3	0.19	50.2
1.5	47.5	670	0.23	53.8	0.20	51.6
1.4	50	700	0.27	57.0	0.24	54.6

- In FY 2014, we will investigate the effects of alternative NSTF catalysts and air management system on system performance and cost.

FY 2013 PUBLICATIONS/PRESENTATIONS

1. X. Wang, R.K. Ahluwalia, X. Wang, and A.J. Steinbach, "Kinetics of Hydrogen Oxidation and Hydrogen Evolution Reactions on Nanostructured Thin-Film Platinum Alloy Catalyst," J. Electrochemical Society, 160 (3) F251-F261, 2013.

2. R.K. Ahluwalia, S. Arisetty, X. Wang, X. Wang, R. Subbaraman, S.C. Ball, S. DeCrane, and D.J. Myers, "Thermodynamics and Kinetics of Platinum Dissolution from Carbon-Supported Electrocatalysts in Aqueous Media under Potentiostatic and Potentiodynamic Conditions," J. Electrochemical Society, 160 (4) F447-F455, 2013.

3. S. Ahmed, D.P. Papadias, and R.K. Ahluwalia, "Configuring a Fuel Cell based Residential Combined Heat and Power System," J. of Power Sources, 242, 884-894, 2013.

4. R.K. Ahluwalia, X. Wang, A. Lajunen, A.J. Steinbach, S.M. Hendricks, M.J. Kurkowski, and M.K. Debe, "Kinetics of Oxygen Reduction Reaction on Nanostructured Thin-Film Platinum Alloy Catalyst," J. of Power Sources, 215 (1) 77-88, 2012.

5. S. Arisetty, X. Wang, R.K. Ahluwalia, R. Mukundan, R. Borup, J. Davey, D. Langlois, F. Gambini, O. Polevaya, and S. Blanchet, "Catalyst Durability in PEM Fuel Cells with Low Platinum Loadings," J. Electrochemical Society, 159 (5) B455-B462, 2012.

6. R.K. Ahluwalia, X. Wang, A. Lajunen, A.J. Steinbach, S.M. Hendricks, M.J. Kurkowski, and M.K. Debe, "Performance of PEFC Stacks with Low-Pt Nanostructured Thin Film Catalysts at High Power Densities," 2012 Fuel Cell Seminar & Exposition, Mohegan Sun, Uncasville, CT, November 5–8, 2012.

7. R.K. Ahluwalia and X. Wang, "Reaction Kinetics and Transport Modeling for Nanostructured Thin Film Catalysts," 4th Transport Working Group Meeting, Lawrence Berkeley National Laboratory, Berkeley, CA, July 26–27, 2012.

8. R.K. Ahluwalia and N. Garland, "Report from the Annexes: Annex 26," IEA AFC ExCo 44th Meeting, Toronto, Canada, June 7–8, 2012.

9. R.K. Ahluwalia, "Fuel Cells for Transportation: Recent Progress in U.S.A.," IEA Annex 26 Meeting, Gothenburg, Sweden, May 22–23, 2012.

REFERENCES

1. M.K. Debe, "Advanced Cathode Catalysts and Supports for PEM Fuel Cells," Grant No. DE-FG36-07GO17007, FreedomCAR Technical Team Review, Detroit, MI, March 10, 2010.

2. A.J. Steinbach, C.V. Hamilton, and M.K. Debe, "Impact of Micromolar Concentrations of Externally-Provided Chloride and Sulfide Contaminants on PEMFC Reversible Stability," ECS Transactions 11(1), 889-897, 2007.

3. R.K. Ahluwalia, X. Wang, A. Lajunen, A.J. Steinbach, S.M. Hendricks, M.J. Kurkowski, and M.K. Debe, "Kinetics of Oxygen Reduction Reaction on Nanostructured Thin-Film Platinum Alloy Catalyst," J. Power Sources, 215, 77-88, 2012.

4. X. Wang, R. K. Ahluwalia, X. Wang, and A. J. Steinbach, "Kinetics of Hydrogen Oxidation and Hydrogen Evolution Reactions on Nanostructured Thin-Film Platinum Alloy Catalyst," J. Electrochemical Society, 160 (3) F251-F261, 2013.

5. R.K. Ahluwalia , X. Wang, J. Kwon, and A. Rousseau, "Drive-Cycle Performance and Life-Cycle Costs of Automotive Fuel Cell Systems," 2011 Fuel Cell Seminar & Exposition, Orlando, FL, October 31 – November 2, 2011.

6. R.K. Ahluwalia, X. Wang, J. Kwon, A. Rousseau, J. Kalinoski, B. James, and J. Marcinkoski, "Performance and Cost of Automotive Fuel Cell Systems with Ultra-Low Platinum Loadings," J. Power Sources, 196, 4619, 2011.

7. B.D. James, J.A. Kalinoski, and K.N. Baum, "Mass Production Cost Estimation for Direct H_2 PEM Fuel Cell Systems for Automotive Applications: 2009 Update," DTI Report GS-10F-0099J, January 2010.